

# Sampling DTI fibers in the human brain based on DWI forward modeling

Song Zhang and David H. Laidlaw

**Abstract**— We present a forward-modeling-based sampling of diffusion-tensor imaging (DTI) integral curves. This work has the potential to generate accurate brain neural fiber models that fit the data well with an economic number of curves.

DTI integral curves are integrated from the first eigenvector field of the DTI field. Usually the seed points are generated randomly or from a regular grid in the data volume. The resulting set of integral curves are dense around the long and skinny neural fiber structures and sparse around the short and fat structures. There is currently a lack of quantitative indication of how well various models fit the data.

We build a forward model that simulates diffusion-weighted images (DWIs) from the DTI integral curves based on a multi-tensor model. We employ the sum of the difference between the simulated DWIs and the acquired DWIs as the goal function and optimize the placement of the DTI integral curves with a greedy algorithm and a simulated annealing algorithm. The results show that with the same number of curves, the optimized set of DTI integral curves fit better to the data than randomly seeded integral curves.

## I. INTRODUCTION

Diffusion tensor imaging reveals neural fiber structures in the brain's white matter [2]. The major eigenvectors of the diffusion tensors point to the direction of the fastest diffusion, which often correlates with the fibrous directions in coherent white matter [7]. Tractography methods track integral curves in the major eigenvector field of the diffusion tensor field in order to generate models that correlate with the underlying anatomy [2].

To generate a set of integral curves that accurately depict the brain white matter anatomy, we need to solve the inverse problems for both generating a single curve and generating a set of curves in the brain white matter volume. The solution for a single integral curve in both coherent and incoherent white matter regions is well-explored by employing high angular resolution [8], regularization [5], Bayesian modeling [4], etc. For the whole-brain model, the placement of the integral curves also affects the quality of the model. This paper proposes a new method for placing an economic set of integral curves that fit the data well.

Previously, Turks and Banks have studied the placement of streamlines to generate an evenly spaced streamline set [9]. We have used a jittered grid sampling combined with distance culling to generate a set of representative streamtubes [11]. Vilanova *et al.* have used a seeding method for 2D steady flow [8] to generate an evenly spaced set of DTI tracts [10].

Song Zhang and David H. Laidlaw are with the Department of Computer Science, Brown University, Providence, RI 02912, USA  
sz,dhl@cs.brown.edu

We extend the idea of image-guided streamline placement [9] to the DTI integral curves. We develop a forward model that generates DWIs from the integral curves with a multi-tensor model. We then use the difference between the simulated DWIs and acquired DWIs to guide the placement of the integral curves. A greedy algorithm and simulated annealing are used to optimize the configuration of the curves.

## II. METHODS

### A. DATA PREPARATION

The Siemens MDDW protocol was used to collect three co-registered sagittal double spin-echo, echo-planar diffusion-weighted volumes of the entire brain. The subject provided written informed consent to participate in a DTI research project approved by the Institutional Review Board at Butler Hospital in Providence, RI.

The volumes were spatially offset in the slice direction by  $0.0mm$ ,  $1.7mm$  and  $3.4mm$ . Parameters for each acquisition were as follows: 5mm thick slices, 0.1mm inter-slice spacing, 30 slices per acquisition,  $matrix = 128 \times 128$ ,  $FOV = 21.7cm \times 21.7cm$ ,  $TR = 7200$ ,  $TE = 156$ , no partial echoes,  $NEX = 3$ . Diffusion encoding gradients ( $b = 0, 1000mm/s^2$ ) were applied in 12 non-collinear directions. The three acquisitions were interleaved to achieve true  $1.7mm^3$  resolution images.

Diffusion tensors were calculated with a non-linear sequential quadratic programming (SQP) method [1].

### B. DTI INTEGRAL CURVES

The integral curves that comprise our tractography models were generated by solving the following equation:

$$p(t) = \int_0^t \vec{v}(p(s)) ds \quad (1)$$

where  $p(t)$  is the generated streamline and  $\vec{v}$  corresponds to the vector field generated from the major eigenvector  $\vec{e}_1$  of the diffusion tensor  $D$ .  $p(0)$  is set to the initial point of the integral curve, often called the seed point. The integration goes into two opposite directions from the seed point.

Given the diffusion tensor field, an integral curve is determined once a seed point is selected.

### C. FORWARD MODELING

We developed a forward model that simulates the DWI signals from the DTI integral curves model and use the difference between the simulated DWIs and acquired DWIs to guide the placement of the integral curves.

The forward-modeling problem in diffusion imaging modeling can be stated as: given the voxel-based partial volume model  $V_p$  and a set of integral curves  $C_i$  representing the coherent neural fiber bundles, how do we get the diffusion MR signal for each voxel in the data volume? We begin by the equation that relates DWI signal to the tensor model [3]:

$$I = I_0 e^{-b:D} \quad (2)$$

$I_0$  is the intensity with no encoding (for a given material type typically a constant within a dataset),  $b$  is the diffusion encoding tensor,  $D$  is the tensor model for the diffusion.

Integrating over a whole voxel, we get:

$$I_v = \int_{\mathbf{x} \in v} I_x d\mathbf{x} = \int_{\mathbf{x} \in v} I_{0x} e^{-b:D_x} d\mathbf{x} \quad (3)$$

To simplify, we make the following assumption:

*Assumption 1:* The diffusion tensor in gray matter or CSF are constant. The diffusion tensor is also constant over any voxel for a single fiber bundle.

With assumptions listed in the last section, we can rewrite equation 3 as:

$$I_v = I_{0csf} e^{-b:D_{csf}} v_{csf} + I_{0gm} e^{-b:D_{gm}} v_{gm} + \sum_i I_{0wm} e^{-b:D_i} v_i \quad (4)$$

$i$  indexes over all the DTI fiber bundles intersecting the voxel. We assume that each fiber bundle is a integral curve with a constant radius; the fiber bundles that intersect  $v$  provide a natural set of coherent white matter compartments.

We segment the brain into white matter  $\sum v_i$ , gray matter  $v_{gm}$  and CSF  $v_{csf}$  compartments using the FAST [12] segmentation tool. We proximate the partial volume for each fiber bundle in a voxel by calculating the distance from the center of the voxel to the fiber bundle curve  $d_i$  and let

$$v_j = \frac{d_j}{\sum_i d_i} \sum_i v_i \quad (5)$$

Assuming that the data measurements are normally distributed around the true value with the same variance, and that the data measurements are independent in different locations, in order to get the maximum likelihood of the data, we need to minimize the quantity:

$$\chi^2 = \sum_{q=1}^m \sum_{v=1}^n \left( \frac{I_{v,q} - \hat{I}_{v,q}}{\sigma} \right)^2 \quad (6)$$

called  $\chi^2$  [6], where  $q$  denotes the set of magnetic gradient directions.  $I$  and  $\hat{I}$  are the scanned and simulated signals.  $\sigma$  is the variance of the distribution of the error between the two signals. We use the noise value in the scanned image for  $\sigma$ .

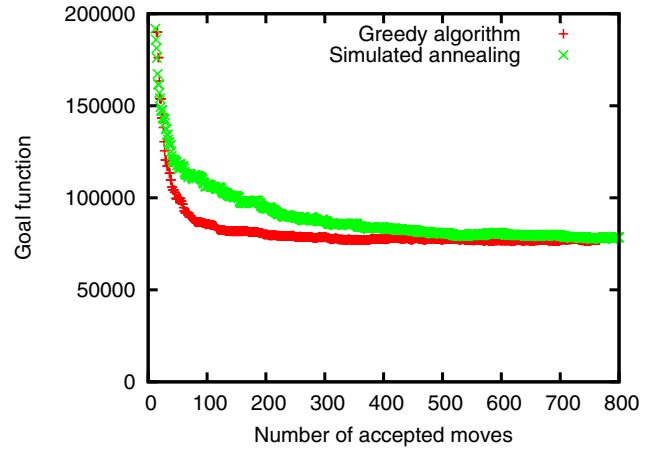


Fig. 1. This plot shows the integral curves optimization processes for the greedy algorithm and the simulated annealing. For both algorithms the  $\chi^2$  value converges to around 77,600. The greedy algorithm converges faster, and it does not appear to get trapped in the local minimum.

#### D. OPTIMIZATION

For a fixed number of DTI integral curves  $N$ , we optimize the configuration of the curves by minimizing the goal function  $\chi^2$ .

We define three kinds of rearrangement:

- Addition: add an integral curve with a randomly selected seed point  $P$ .
- Removal: remove a randomly selected integral curve  $C$  from the current configuration.
- Addition and removal: a combination of one addition and one removal.

The  $\chi^2$  difference  $\Delta\chi^2 = \chi_2^2 - \chi_1^2$  is calculated after each step.

The greedy algorithm works as follows:

- 1) If the number of curves is less than  $N$ , try addition. If  $\Delta\chi^2 < 0$ , accept the addition.
- 2) If the number of curves is equal to  $N$ , try addition and removal. If  $\Delta\chi^2 < 0$ , accept the addition and removal.
- 3) Repeat 2 until the decrease in  $\chi^2$  becomes discouraging.

To avoid the local minimum, we also implemented a simulated annealing algorithm as follows:

- 1) If the number of curves is less than  $N$ , try addition. If  $\Delta\chi^2 < 0$ , accept the addition. If  $\Delta\chi^2 \geq 0$ , accept with probability  $\exp(\frac{-\Delta\chi^2}{kT})$ .
- 2) If the number of curves is equal to  $N$ , try addition and removal. If  $\Delta\chi^2 < 0$ , accept the addition and removal. If  $\Delta\chi^2 \geq 0$ , accept with probability  $\exp(\frac{-\Delta\chi^2}{kT})$ .
- 3) Repeat 2 until the number of reconfigurations reaches  $N_R$  or the number of steps reaches  $N_S$ . Reduce  $T$  by 10% if any of the two conditions are met.
- 4) Repeat 3 until  $T$  becomes close to 0.

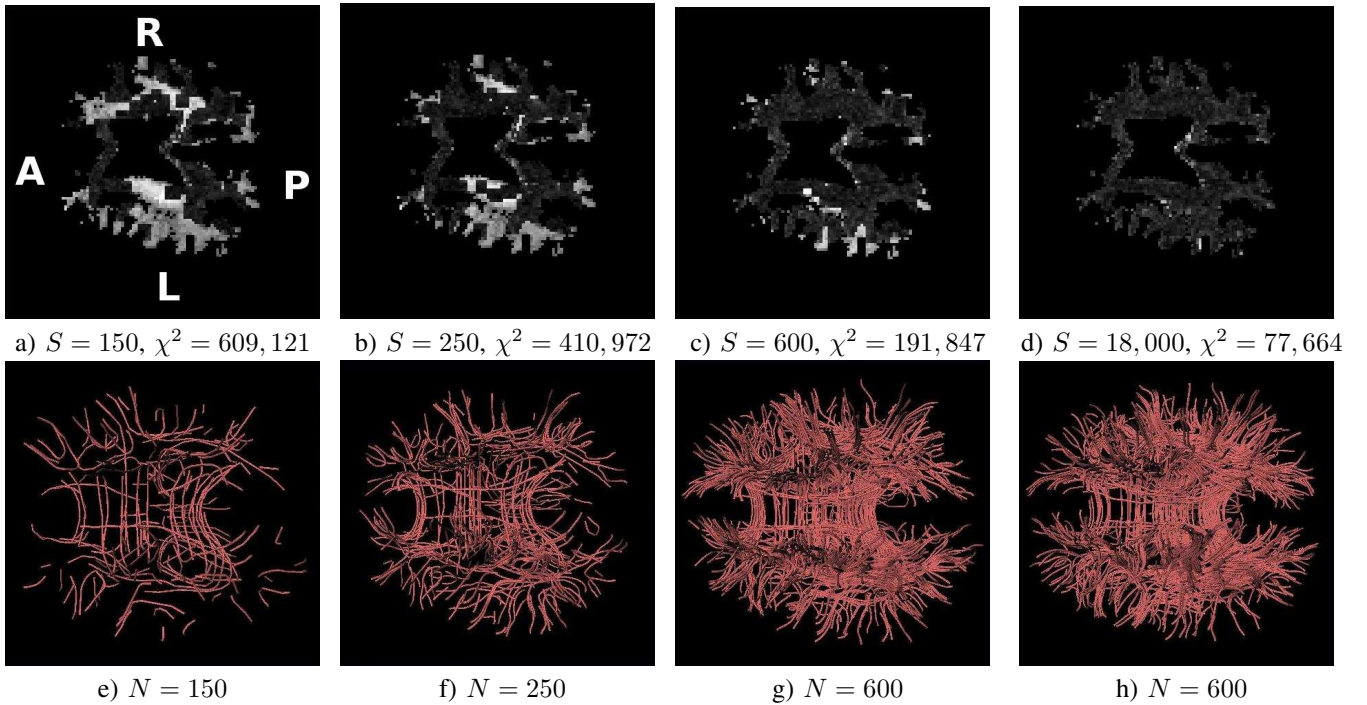


Fig. 2. a), b), c) and d) show the snapshots of the value  $\chi_v^2 = \sum_{q=1}^m \left( \frac{I_{v,q} - \hat{I}_{v,q}}{\sigma} \right)^2$  for each voxel  $v$  in the data volume during different stages of the simulated annealing.  $S$  is the number of accepted moves. e), f), g) and h) show the integral curves model generated at these stages.  $N$  is the number of curves. Note that g) and h) both have 600 curves, but the optimization of the configuration lowered the  $\chi^2$  value from g) to h) significantly.

### III. RESULTS AND DISCUSSION

We ran the two optimization algorithms on the brain data set. Since we are interested in the white matter structures, we limit our  $\chi^2$  calculation to the voxels with more than 50% white matter. There are 84,025 such voxels. The seed points for a new integral curve were selected within these voxels. We set the target number of the curves to 600. The  $k$  in simulated annealing was set to 1. The temperature  $T$  was originally set to 1000.  $N_R$  was set to 300 and  $N_S$  was set to 600.

Fig. 1 shows the optimization processes for the greedy algorithm and the simulated annealing. For both algorithms the  $\chi^2$  value converges to around 77,600. The greedy algorithm converges faster, and it does not appear to get trapped in the local minimum.

Fig. 2 shows the snapshots of the value  $\chi_v^2 = \sum_{q=1}^m \left( \frac{I_{v,q} - \hat{I}_{v,q}}{\sigma} \right)^2$  for each voxel  $v$  in the data volume during different stages of the simulated annealing. While the addition of the curves quickly fills in large high  $\chi_v^2$  area, the repeated addition and removal steps gradually decrease the overall  $\chi^2$  value by reconfiguration.

For comparison, we also performed random seed point sampling for generating 600 integral curves and calculated  $\chi^2$  values for these models. The experiment was repeated five times and  $\chi^2 = 197,840 \pm 9,166$ .

### IV. CONCLUSIONS AND THE FUTURE WORK

We present a forward-modeling-based sampling of diffusion-tensor imaging (DTI) integral curves. We build a

forward model that generates DWIs from the DTI integral curves based on multi-tensor modeling. We employ the sum of the difference between the simulated DWIs and the acquired DWIs as the goal function and optimize the placement of the DTI integral curves with a greedy algorithm and a simulated annealing approach. The results show that with the same number of curves, the optimized set of DTI integral curves fit better to the data than randomly seeded integral curves. With the proposed moves of random addition, random removal and their combination, the greedy algorithm converges faster and does not seem to get trapped in local minimums.

This work has the potential to generate accurate representation of the white matter anatomy with economic number of curves.

Note that we made several simplifications in our forward model such as the white matter partial volumes calculation, or the constant radius of the fiber bundles. Future improvement on the precision of the forward model may help increase the accuracy of the optimized model.

### V. ACKNOWLEDGMENTS

This work was partially supported by US National Science Foundation (CCR-0086065), US National Institutes of Health (NIH EB004155), and the Brain Science Program at Brown.

### REFERENCES

- [1] Eric T. Ahrens, David H. Laidlaw, Carol Readhead, Celia F. Brosnan, and Scott E. Fraser. MR microscopy of transgenic mice that spontaneously acquire experimental allergic encephalomyelitis. *Magnetic Resonance in Medicine*, 40(1):119–132, July 1998.

- [2] Peter J. Basser, Sinisa Pajevic, Carlo Pierpaoli, Jeffrey Duda, and Akram Aldroubi. In vivo fiber tractography using DT-MRI data. *Magnetic Resonance in Medicine*, 44:625–632, 2000.
- [3] P.J. Basser, J. Mattiello, and D. LeBihan. Estimation of the effective self-diffusion tensor from the NMR spin echo. *Journal of Magnetic Resonance, Series B*, 103(3):247–54, March 1994.
- [4] T.E.J. Behrens, M.W. Woolrich, M. Jenkinson, H. Johansen-Berg, R.G. Nunes, S. Clare, P.M. Matthews, J.M. Brady, and S.M. Smith. Characterization and propagation of uncertainty in diffusion-weighted mr imaging. *Magnetic Resonance in Medicine*, 50:1077–1088, 2003.
- [5] C. Poupon, C. A. Clark, V. Frouin, J. Regis, I. Block, D. Le Behan, and J.-F. Mangin. Regularization of diffusion-based direction maps for the tracking of brain white matter fascicles. *NeuroImage*, 12:184–195, 2000.
- [6] William H. Press, Saul A. Teukolsky, William T. Vetterling, and Brian P. Flannery. *Numerical Recipes in C: The Art of Scientific Computing*. Cambridge University Press, New York, New York, second edition, 1992.
- [7] D.F. Scollan, A. Holmes, R. Winslow, and J. Forde. Histological validation of myocardial microstructure obtained from diffusion tensor magnetic resonance imaging. *American Journal of Physiology*, 275:2308–2318, 1998.
- [8] D.S. Tuch, R.M. Weisskoff, J.W. Belliveau, and V.J. Wedeen. High angular resolution diffusion imaging of the human brain. In *Proceedings of the 7th Annual Meeting of ISMRM*, page 321, 1999.
- [9] G. Turk and D. Banks. Image-guided streamline placement. In *Proceedings of SIGGRAPH 96*, pages 453–460. ACM SIGGRAPH, 1996.
- [10] A. Vilanova, G. Berenschot, and C. van Pul. DTI visualization with streamsurfaces and evenly-spaced volume seeding. In *VisSym '04 Joint Eurographics - I.E.E.E. T.C.V.G. Symposium on Visualization, Conference Proceedings*, pages 173–182, 2004.
- [11] Song Zhang, Cagatay Demiralp, and David H. Laidlaw. Visualizing diffusion tensor MR images using streamtubes and streamsurfaces. *IEEE Transactions on Visualization and Computer Graphics*, 9(4):454–462, October 2003.
- [12] Y. Zhang, M. Brady, and S. Smith. Segmentation of brain mr images through a hidden markov random field model and the expectation maximization algorithm. *IEEE Transactions on Medical Imaging*, 20(1):45–57, 2001.